

Curvature, slip, and viscosity in ^3He - ^4He mixtures

Sorin Perisanu and Gerard Vermeulen*

Centre de Recherche sur les Très Basses Températures, CNRS, Boîte Postale 166, 38402 Grenoble Cédex 9, France

(Received 25 January 2006; published 24 April 2006)

We report vibrating wire viscometer experiments in the concentrated and dilute phase of saturated ^3He - ^4He mixtures showing that the slip length may become orders of magnitude larger than the mean free path due to specular scattering of the ^3He quasiparticles with a ^4He coating adsorbed at the surface of the wire. Since the liquid does not almost stick to the surface, the boundary conditions for fluid flow are unusual and not accounted for by the current theory for slip [H. Højgaard Jensen *et al.*, *J. Low Temp. Phys.* **41**, 473 (1980)]. The experimental results are in excellent agreement with a recent theory for slip [R. Bowley and J. Owers-Bradley, *J. Low Temp. Phys.* **136**, 15 (2004)] which accounts for the effect of the cylindrical geometry and for velocity slip in directions normal as well as tangential to the surface of the wire. We find that our viscosity measurements in the dilute phase resulting from the data analysis based on the recent slip theory are in better agreement with the Fermi liquid theory than previous experimental results.

DOI: [10.1103/PhysRevB.73.134517](https://doi.org/10.1103/PhysRevB.73.134517)

PACS number(s): 67.55.Fa, 47.45.Gx, 67.60.Fp

I. INTRODUCTION

The hydrodynamic equations describing fluid flow near a solid wall are usually solved assuming that the relative velocity between the fluid and the solid is zero at the surface of the wall. The assumption is known as the no-slip boundary condition and has been successfully applied in the description of many experiments. The no-slip boundary condition for the velocity normal to the wall is a direct consequence of zero mass current across the wall. However, the no-slip condition for the velocity tangential to the wall is justified by microscopic arguments which break down in certain circumstances. In a dilute gas, for instance, the extrapolation of the tangential fluid velocity towards the surface matches that of the surface only some distance ζ behind it. This phenomenon is known as slip and is described with a boundary condition relating the tangential velocity to its derivative normal to the surface, $v_t = \zeta \partial v_t / \partial n$. The relation between the slip length ζ and the mean free path l depends on the nature of the scattering of the fluid particles with the wall; $\zeta/l \sim 1$ in the case of diffusive scattering and $\zeta/l \rightarrow \infty$ in the case of specular scattering. Slip has also been observed in dense liquids, where it is affected by the molecular interactions between the fluid and the solid, by wetting or nonwetting, and by surface roughness.

Slip is very temperature dependent in pure liquid ^3He and ^3He - ^4He mixtures at low temperatures, because those systems behave like degenerate Fermi liquids with a viscous mean free path $l_\eta \propto T^{-2}$. A slip length of order $10 \mu\text{m}$ is easily attainable. Moreover, pure ^3He has a superfluid transition temperature of about 1 mK and far below that temperature the density of excitations becomes very low and the system enters the ballistic regime. Torsional oscillator experiments in ^3He - ^4He mixtures and pure ^3He have shown a strong enhancement of the slip length due to specular scattering of the ^3He quasiparticles off a superfluid ^4He film preferentially adsorbed on the wall.¹⁻³ The enhancement of the slip length is not yet understood, but the superfluidity of the adsorbed ^4He layers does play a role.³ However, vibrat-

ing wire viscometer experiments in dilute ^3He - ^4He mixtures spanning the transition from the hydrodynamic to the ballistic regime have been practically unaffected by specular scattering.⁴⁻⁶

In this paper, we report vibrating wire viscometer experiments showing that the slip length may become much larger than the radius of the wire a , while the liquid is still in the hydrodynamic regime ($l_\eta \ll a$). The liquid does almost not stick to the wire and the current theory for slip⁷ based on (1) the slip boundary condition for a flat surface and (2) the hydrodynamic boundary condition of zero radial liquid velocity at the surface of the wire is stretched beyond its validity limits. We find good agreement with a recent theory for slip⁸ characterized by (1) a slip condition for a curved surface allowing slip of the tangential *and* the radial velocity at the surface of the wire and (2) a boundary condition for the radial velocity obtained from the equality between a hydrodynamic and a microscopic expression for the force on the wire.

The original motivation for this work was to calibrate vibrating wire viscometers in ^3He - ^4He mixtures for thermometry purposes at temperatures in the range of 10–100 mK and magnetic fields up to 11.5 T. We show that the theory of Bowley and Owers-Bradley⁸ is necessary to resolve the apparent initial inconsistency in the results obtained with wires of different diameters and to determine the viscosity correctly. Preliminary reports of this work have been published elsewhere.^{9,10}

II. BACKGROUND

A. Introduction

The viscometers are made of a wire bent and glued into a support to form a freestanding semicircle. The device is oriented in a static magnetic field such that the Lorentz force on a current passing through the wire is zero at the end points of the semicircle and maximal at the middle. An alternating current through the wire produces a flapping motion of the

wire out of its plane. The frequency of the current is swept through the mechanical resonance and the oscillation is detected by measuring the induced voltage across the wire. When the viscometer is immersed, the resonant frequency shifts and the resonance width broadens because the surrounding liquid exerts an inertial and a damping force on the wire.

The forces have been calculated by Stokes in the hydrodynamic regime for a straight oscillating cylinder from the velocity field which is the solution of the linearized Navier-Stokes equation. The velocity field depends on two integration constants which are determined by the boundary conditions for the r and ϕ component of the velocity in the rest frame of the wire, $v_r(a) = v_\phi(a) = 0$, where a is the radius of the wire. The inertial and the damping force are proportional to the real and imaginary part of the Stokes coefficient $k(m)$, where $m = a/\delta\sqrt{2}$ with δ as the viscous penetration depth.^{7,11,12}

Stokes' solution is easily generalized to superfluids with an isotropic gap such as superfluid ³He-*B* or two component systems consisting of normal ³He dissolved in superfluid ⁴He. Those superfluids consist of a normal component with a density ρ_n and a superfluid component with a density ρ_s . The superfluid component contributes only to the inertial force and the normal component contributes to the inertial and damping forces, parametrized by the viscous penetration depth, $\delta = \sqrt{2\eta/\rho_n\omega} = \sqrt{2\nu/\omega}$ where η is the viscosity, ν is the kinematic viscosity, and ω is the angular frequency of the wire.

The hydrodynamic forces on a straight cylinder are a good approximation to the forces on a semicircular loop as long as the viscous penetration depth is much smaller than the radius of the loop. This is the case in our experiments, since the radius of the loop is 2 mm or more and the viscous penetration depth is 50 μm or less.

B. Slip and boundary conditions

Slip changes the boundary conditions for the velocity field, and therefore $k(m)$ and the resonance shift and width. Høgaard Jensen *et al.*⁷ have derived a modification of the complex Stokes coefficient using the slip condition for a flat surface $v_r = \zeta \partial v_r / \partial n$ and the condition $v_r(a) = 0$,

$$k_i(m, \beta) = 1 + \frac{1}{(k(m) - 1)^{-1} - im^2\beta}, \quad (1)$$

where

$$\beta = \frac{\zeta}{\zeta + a}, \quad (2)$$

$$\zeta = 0.5819 \frac{1+s}{1-s} l_\eta, \quad (3)$$

a is the radius of the wire, s is the fraction of specular reflections, and l_η is related to the viscosity by the Fermi liquid relation $\eta = \rho_n \nu = \frac{1}{5} n_3 p_F l_\eta$. Equation (1) is valid as long as $\zeta \ll a$. We will present experimental data in pure ³He which is in good agreement with this description and data in mixtures

showing that the theory is stretched beyond its validity range when $\zeta \approx a$.

A simple argument shows that the slip boundary condition $v_r = \zeta \partial v_r / \partial n$ does not account for the curvature of the wire in case of full specular scattering.⁸ When $s=1$, the ³He quasiparticles are reflected from the wire such that there is no transfer of tangential momentum between the wire and the quasiparticles. Therefore, the $r\phi$ component of the momentum flux tensor given by

$$\Pi_{r\phi}(r, \phi) = -\eta \left(\frac{\partial v_\phi}{\partial r} + \frac{1}{r} \frac{\partial v_r}{\partial \phi} - \frac{v_\phi}{r} \right)$$

vanishes at the surface of the wire. Here v_r and v_ϕ are the components of the velocity of the liquid in cylindrical coordinates. Application of the boundary condition $v_r(a) = 0$ in the rest frame of the wire gives

$$\left(\frac{\partial v_\phi}{\partial r} \right)_{r=a} - \frac{v_\phi(a)}{a} = 0. \quad (4)$$

The solution of the Navier-Stokes equation with this boundary condition gives Eq. (1) with $\beta=1/2$ instead of $\beta=1$ obtained by naive substitution of $s=1$ in Eq. (2).

In view of the above argument, it is reasonable to define the slip length as $\Pi_{r\phi}(a, \phi) \equiv -\eta v_\phi(a, \phi) / \zeta$ which leads using the condition $v_r(a) = 0$ to

$$\left(\frac{\partial v_\phi}{\partial r} \right)_{r=a} - \frac{v_\phi(a)}{a} = \frac{v_\phi(a)}{\zeta}, \quad (5)$$

a result found by Einzel *et al.*¹³ Equation (5) reduces to the slip condition for a flat surface in the limit $\zeta \ll a$. Einzel *et al.* interpret $(1/v_\phi(a))(\partial v_\phi / \partial r)_{r=a}$ as the slip length, so that the slip length contains the curvature of the wire and the scattering of the quasiparticles off the surface. We prefer to analyze our data in terms of ζ which characterizes the physics at the surface and we call ζ the slip length. Of course, $v_\phi(r)$ still extrapolates to zero at the center of the cylinder when $\zeta \rightarrow \infty$. The solution of the Navier-Stokes equation with Eq. (5) as a boundary condition results in Eq. (1) with β given by

$$\beta = \frac{\zeta}{2\zeta + a}. \quad (6)$$

The inadequacy of the hydrodynamic description of the liquid within a few viscous mean free paths from the wire manifests itself when the viscous mean free path l_η becomes comparable to the radius of the wire a . The microscopic radial velocity at the surface of the wire is still zero because the number of quasiparticles is conserved but the extrapolation of the hydrodynamic radial velocity to $r=a$ —well defined a few mean free paths away from the surface of the wire—is not necessarily zero.

Bowley and Owers-Bradley⁸ have solved the Boltzmann equation to calculate the momentum flux tensor which is used in the derivation of two improved boundary conditions. The theory is valid as long as $l_\eta \ll a$ and $s \rightarrow 1$ because it neglects terms of order l_η/a and higher and nonspecular scattering.

The first slip boundary condition follows from the argument that $\Pi_{r\phi}$ is constant for values of $(r-a)$ which are small compared to the radius a ,⁸

$$\left(\frac{\partial v_\phi}{\partial r}\right)_{r=a} + \frac{1}{a} \frac{\partial v_r(a)}{\partial \phi} - \frac{v_\phi(a)}{a} = \frac{v_\phi(a)}{\zeta}, \quad (7)$$

where the condition $v_r(a)=0$ has been relaxed. The theory also predicts that Eq. (3) remains valid for a cylindrical geometry.⁸

The momentum flux tensor obtained from the Boltzmann equation also permits us to calculate the force exerted by the liquid on the wire. On the other hand, the hydrodynamic theory permits to evaluate the force exerted on an annulus of liquid with a thickness of a few mean free paths surrounding the wire. When the mean free path is much smaller than the viscous penetration depth, the hydrodynamic force on the annulus is approximately equal to the force on the surface of the wire. Equality of the force exerted by the liquid on the wire calculated from the solution of the Boltzmann equation and from hydrodynamic theory provides the second boundary condition.⁸

Both boundary conditions permit us to eliminate the integration constants in the solution of the Navier-Stokes equation and lead to a modified Stokes coefficient which accounts for tangential and radial slip,

$$k_{tr}(m, \beta) = \frac{1}{\frac{1+3s}{4} - \Phi} \times \left(\frac{3+s}{4} + \frac{\left(\frac{1+3s}{4} - \frac{1-s}{2(k(m)-1)}\right)(1+\Xi)}{\frac{1}{k(m)-1} - \frac{\left(\frac{1+3s}{4} - \Phi\right)im^2\beta}{\frac{1+s}{2} - \Phi + \frac{1-s}{2}\beta} - \Xi} \right), \quad (8)$$

where $\Xi = -(2\beta+1)\Phi/(2\Phi+(s-1)\beta-s-1)$, $\Phi = 4ia\rho_n\omega/3n_3p_F = 16im^2l_\eta/15a$, n_3 is the number density of ${}^3\text{He}$ atoms, and p_F is the Fermi momentum. We emphasize, that $k_{tr}(m, \beta)$ has *a priori* only two unknown independent parameters because β , s , and $m=(a/2)\sqrt{\omega/\nu}$ are related through the Fermi liquid expression $\eta = \rho_n\nu = \frac{1}{5}n_3p_F l_\eta$ and because Φ depends on the frequency, known properties of the liquid, and the radius of the wire.

C. Viscometer

The equation of motion for a semicircular vibrating wire resonator differs from that for a damped harmonic oscillator and the response of the resonator is not perfectly Lorentzian. The deviations from a Lorentzian are clearly visible at low quality factors. The viscometer response is better described by an equation due to Carless *et al.*¹² which we have adapted to account for the ohmic resistance and the intrinsic damping of the wire,

$$Z = X + iY = R + \frac{R_v z_0^4}{\pi^4 - z^4} f(z), \quad (9)$$

where $R_v = i\omega B^2 L / 2\omega_w \pi a^2 \rho_w$,

$$f(z) = 1 + \frac{4\pi^2 z (\sinh z(1 + \cos z) - \sin z(1 + \cosh z))}{(\pi^4 - z^4)(1 - \cos z \cosh z)}$$

and

$$z^4 = z_0^4 \frac{\omega^2}{\omega_w^2} \left[1 + \frac{i\omega_w}{Q_w \omega} + \frac{\rho_s}{\rho_w} + \frac{\rho_n}{\rho_w} k_{tr}(m, \beta) \right]. \quad (10)$$

Here $z_0 \approx 4.73004$ is the first zero of $1 - \cos z \cosh z$, ω_w and Q_w are the resonance angular frequency and the quality factor of the first mechanical resonance of the wire in vacuum, ρ_w is the density of the wire, B is the magnetic field, and L and R are the length of the wire and its ohmic resistance. Since the shape of the response of the vibrating wire resonator is not Lorentzian, the resonance width $f_+ - f_-$ and resonance frequency f_0 need to be explicitly defined:¹² f_0 is given by $Y(f_0) \equiv 0$ and f_+ and f_- are given by $X(f_\pm) - R \equiv \pm Y(f_\pm)$.

We consider the limit $s \rightarrow 1$ to discuss the effect of Eq. (8) on the response of the viscometer. In this limit, Eq. (8) simplifies to⁸

$$k_{tr}(m, \beta) \approx \frac{1}{1 - \Phi} \left[1 + \frac{1 + \Phi}{(k(m) - 1)^{-1} - im^2\beta - \Phi} \right], \quad (11)$$

since $\Xi \approx \Phi/(1 - \Phi) \approx \Phi$. At high temperature, Φ is negligible and Eq. (11) reduces to Eq. (1) [with Eq. (6)] which describes tangential slip enhanced by specular scattering. Although $|\Phi|$ is much smaller than 1, the importance of the Φ term in the denominator between the brackets increases towards lower temperatures, because $m \rightarrow 0$, $k(m) \rightarrow \infty$, and Φ is temperature independent. The Φ term arises from the radial slip and describes the Knudsen regime. At very low temperatures, Eq. (11) is pushed beyond its validity region since $l_\eta > a$, but Eq. (11) still manifests ballistic behavior. In the ballistic limit, the resonance width is given by $f_+ - f_- = 3n_3 p_F / 8\pi a \rho_w$ while the shift of the resonance frequency is unaffected by ρ_n , since $k_{tr} \approx -1/\Phi$ is imaginary and since the shift and the width⁴ are given by $f_0 - f_{\text{ideal}} = (\rho_n / 2\rho_w)(k'_{tr} - 1)f_0$ and $f_+ - f_- = (\rho_n / \rho_w)k''_{tr}f_0$, where $k_{tr} = k'_{tr} + ik''_{tr}$. By kinetic arguments the width is expected to be $f_+ - f_- = An_3 p_F / (2\pi^2 a \rho_w)$ where Bowley has estimated $A \approx 2.36$ for elastic scattering on a smooth wire.¹⁴ This value is practically equal to the value extrapolated from Eq. (11): $A = 3\pi/4$.

III. EXPERIMENTAL SETUP AND DATA ANALYSIS

The experimental setup has been designed to measure the temperature dependence of the viscosity of ${}^3\text{He}$ - ${}^4\text{He}$ mixtures in high magnetic field. A total of eight viscometers has been placed inside two cells containing saturated ${}^3\text{He}$ - ${}^4\text{He}$ mixtures with the concentrated phase (almost pure ${}^3\text{He}$) floating on top of the dilute phase. The first cell for experiments at SVP is the mixing chamber of a ${}^3\text{He}$ - ${}^4\text{He}$ dilution refrigerator with two viscometers at the top in the concen-

trated phase and two viscometers at the bottom in the dilute phase. The second cell for experiments at pressures in the range of 0–20 bars contains also two viscometers at the top and two viscometers at the bottom. This cell has been mounted below the mixing chamber on a silver rod thermally anchored to the mixing chamber. A ^3He melting curve thermometer¹⁵ and a Coulomb blockade thermometer¹⁶ have been mounted on the silver rod. The whole setup has been placed inside a 12 T magnet and we have varied the field between 4 and 11.5 T to verify that the slip effects are not field dependent. The lowest temperature in the second cell is about 15 mK due to an unidentified heat leak to the silver rod. The Coulomb blockade thermometer is operational down to about 40 mK and the melting curve thermometer in the whole temperature range although the thermal time constants are on the order of 1 h at the lowest temperature because of the high magnetic field.

We have continued to monitor viscometers in the mixing chamber of the ^3He - ^4He dilution refrigerator in completely different experiments. Our most pronounced results on slip have been obtained in those experiments because of the lower temperatures (down to below 6 mK).

The viscometers have been made out of ϕ 25.7 μm PtRh wire and ϕ 62.2 μm CuNi wire with nominal densities of 17 520 and 6 658 kg/m^3 . The radius of the wires has been measured with a normal microscope and an electron beam microscope. The density has been calculated from the mass of a piece of wire of 1 m length. We have also checked the mechanical properties of the wires by experiments in superfluid ^4He at temperatures below 50 mK. The superfluid ^4He acts as an ideal liquid and we have calculated the density of the wire from the shift of the resonance frequency with respect to vacuum: $\omega_{\text{ideal}} = \omega_w \sqrt{\rho_w / (\rho_w + \rho_s)}$. Both determinations of the wire density agree to within 1%.

The experimental errors in the slip measurements depend to a large extent on the errors in the measurements of the shift of the resonance frequency with respect to its vacuum value and on the uncertainties in the values for the densities of the liquid and the wire. We have worked without high frequency filters on top of the cryostat and have disabled the internal filters of the digital lock-in amplifier to eliminate errors in the frequency measurements due to spurious phase shifts. The advantage of resistive viscometers in high field with respect to superconducting viscometers in low field is that the contribution of the self-inductance of the wire to the total impedance is negligible with respect to the resistance of the wire and the impedance due to the mechanical motion of the wire in the magnetic field (both are never lower than 5 Ω). Grounding a current and a voltage terminal at the top of the cryostat eliminates practically all phase shifts induced by the twisted wires between the viscometers and the top of the cryostat. Measurement of the Ohmic resistance of the viscometers at zero field in the frequency range 0.1–10 kHz shows that the phase shift is less than 0.1° . The resonance frequency and the quality factor, ω_w and Q_w of the viscometers in vacuum depend on temperature and magnetic field. The characterization of the viscometers in the high pressure cell is done at temperatures below 100 mK, but vacuum measurements of the viscometers in the mixing chamber are only possible at temperatures above 2–3 K. We have cor-

rected the value of ω_w for each wire by a constant shift in the data analysis when needed; typically 0.05–1.0 Hz for the wires in the mixing chamber and less for the wires in the experimental cell. Eddy currents reduce the values for Q_w to about 6000–8000 in a field of 11.5 T.

A computer program controls the temperature and sweeps the frequency of the excitation current of the viscometers over an interval centered on the resonance frequency to measure the in- and out-phase component of the voltage over the wire. At the lowest temperatures, we have used excitation currents in the range 0.1–0.4 A for voltages over the viscometers at resonance in the range 10–20 V.

Fits of Eq. (9) with Eqs. (10) and (8) to the viscometer response result in four independent parameters: ν (or l_η) and β characterizing the kinematic viscosity (or the mean free path) and the slip length, and R and R_v characterizing the vibrating wire. A polynomial fit¹⁷ to data of the density of pure ^3He as a function of pressure has been used in the analysis of the measurements in the concentrated phase and in pure ^3He . The analysis of the dilute phase measurements requires values for the normal and superfluid density which have been calculated from the relation $v_m(T, p, x) = v_4(p)[1 + \alpha(x, p, T)x]$ and the quasiparticle effective mass, where v_m is the molar volume of a mixture of concentration x at pressure p and temperature T , v_4 is the molar volume of pure ^4He , and α measures the difference in volume occupied by a ^4He and a ^3He atom. We have used the results for $\alpha(p, T=0)$ and $v_4(p)$ published by Watson *et al.*,¹⁸ our fit of the form $x_s(p, T) = x_s(p, T=0)[1 + \beta_2(p)T^2 + \beta_3(p)T^3]$ to the measurements of the saturation concentration by Yorozu *et al.*,¹⁹ and a fit by Rodrigues *et al.*²⁰ to data of the effective mass as a function of pressure in the dilute phase.

The parameters ν , β , R , and R_v have been substituted in Eq. (9) to find the shift of the resonance frequency $f_0 - f_{\text{ideal}}$ and resonance width $f_+ - f_-$.

IV. SLIP RESULTS

The effect of the superfluid ^4He film on the wall is shown in Fig. 1. It shows a comparison of the relation between resonance shift and resonance width for the same PtRh wire in concentrated ^3He and in nominally 99.995% pure ^3He over almost the same temperature range. The pure ^3He data shows a little bit of slip and is in good agreement with Eq. (1) and $(1+s)/(1-s) = 2.2$. The values for $(1+s)/(1-s)$ measured by the CuNi viscometers in pure liquid ^3He fall in the range 1.0–1.1. The concentrated phase data shows much more slip and we attribute the slip to enhanced specular scattering of the ^3He quasiparticles off the superfluid ^4He film adsorbed on the wire.

The analysis based on the theory of Høgaard Jensen *et al.*⁷ of the concentrated phase data yields viscosity results in agreement with measurements of the viscosity in pure ^3He .¹² However, the results for β are incompatible with Eq. (2) and a constant value for the specular scattering fraction. We find that the concentrated phase data is close to the calculation with $\beta = 1/2$ which assumes full specular scattering and takes the curvature of the wire into account. The difference between the data and the calculation with $\beta = 1/2$ is explained

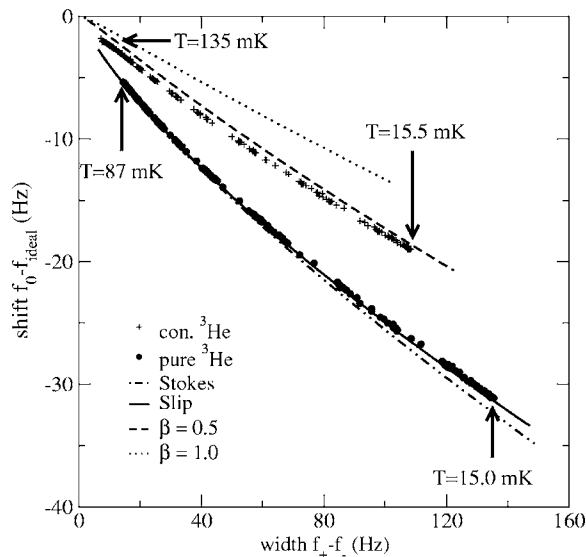


FIG. 1. The comparison of the shift of the resonance frequency versus the resonance width of the same PtRh viscometer in concentrated ${}^3\text{He}$ and 99.995% pure ${}^3\text{He}$ shows that the curvature of the wire has to be included in the slip boundary condition when $\zeta \sim a$. f_{ideal} is the resonance frequency of the wire in a zero viscosity fluid with the density of liquid ${}^3\text{He}$ at $T=0$ K ($f_w=1481.38$ Hz and $f_{\text{ideal}}=1477.88$ Hz). Also shown are calculated curves based on the solution of the Navier-Stokes equation (dashed-dotted line), on Eq. (1) with $(1+s)/(1-s)=2.2$ (full line) and with $\beta=1$ (dotted line), and $\beta=1/2$ (dashed line).

by a finite value for $(1+s)/(1-s)$. The behavior of the concentrated phase is very unusual; the flow is still hydrodynamic since $l_\eta/a \leq 0.01$ but the limit of complete tangential slip is almost reached.

The analysis using Eq. (8) of data taken with a PtRh wire in the dilute phase at SVP in the temperature range 5.5–100 mK results in the relation between the slip coefficient β and the mean free path l_η shown in Fig. 2. The agreement between the experimental results and Eq. (6) with $(1+s)/(1-s)=100$ is excellent for $l_\eta < 5 \mu\text{m}$. The small discrepancy between theory and experiment for $l_\eta > 5 \mu\text{m}$ is insignificant because the theory of Bowley and Owers-Bradley⁸ assumes $l_\eta/a \ll 1$.

Figure 3 shows the same experimental results as resonance shift versus resonance width. The full curve has been calculated on basis of Eq. (8) with $(1+s)/(1-s)=100$ and $\Phi=0.00345i$, where Φ has been calculated from the number density and the effective mass of the ${}^3\text{He}$ atoms in the dilute phase and the frequency. At temperatures close to 100 mK the data falls between the curves representing the solution of Stokes (dashed-dotted line, $\beta=0$) and the solution assuming full specular scattering (dashed line, $\beta=1/2$). This reflects itself in the finite value for $(1+s)/(1-s)$ resulting from the data analysis. The radial slip explains why the data falls above the solution assuming full specular scattering at lower temperatures.

Finally, we did not need to adjust the resonance frequency of the wire in vacuum f_w for this data set but comment on the possible consequences: a small constant shift of f_w by 0.05 Hz would shift the theoretical curves in Fig. 3 by the

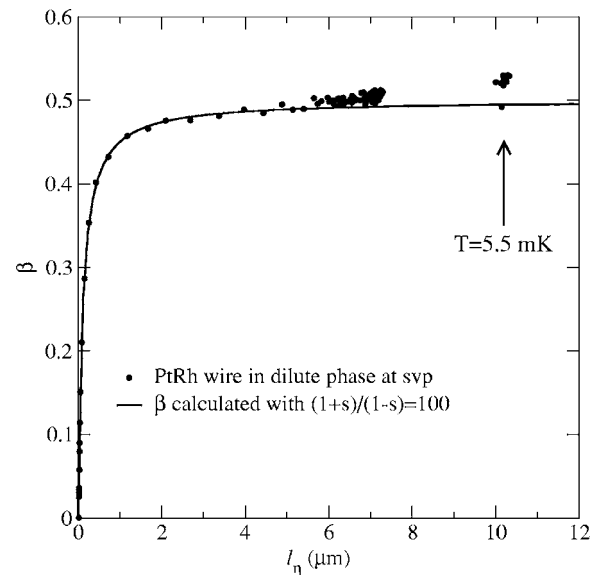


FIG. 2. The slip coefficient $\beta=\zeta/(2\zeta+a)$ versus the viscous mean free path l_η measured with a PtRh wire in the dilute phase at svp. The agreement between the results based on Eqs. (10) and (8) for $l_\eta < 5 \mu\text{m}$ ($l_\eta/a < 0.4$) and the calculation of β with $(1+s)/(1-s)=100$ is excellent.

same amount in the vertical direction. However, it would have a significant effect on the experimental results of β versus l_η shown in Fig. 2 in the region $l_\eta < 2 \mu\text{m}$, in any case larger than the discrepancy between the data and the calculated curve at $l_\eta \approx 10 \mu\text{m}$. The results for $(1+s)/(1-s)$ are thus very sensitive to the errors in f_w .

Figures 1 and 2 of Perisanu and Vermeulen¹⁰ show the results for shift versus width measured by another PtRh wire in the concentrated and dilute phase from 7 to about 100 mK at 0 bar. Fits to this data for β versus l_η give $(1+s)/(1-s) \approx 2500$ in the concentrated phase and $(1+s)/(1-s) \approx 350$ in the dilute phase. The agreement between this data and the theory of Bowley and Owers-Bradley is very good. We emphasize the effect of the radial slip in the concentrated phase is much smaller than in the dilute phase because l_η is smaller.

We do not know why the specular scattering fraction is lower in the dilute phase ($s \approx 0.994$) than in the concentrated phase ($s \approx 0.9992$). The specular enhancement factor $(1+s)/(1-s)$ is always an order of magnitude larger in the concentrated phase than in the dilute phase, although $(1+s)/(1-s)$ may be up to 5 times as low in a particular phase for other viscometers made out of the same wire. We can think of two differences between the concentrated phase and the dilute phase which could give a clue for an explanation for the difference in s : (1) in the dilute phase the concentration changes from zero at the surface of the wire to its bulk value at some distance away while in the concentrated phase the wire is surrounded by a thin layer of dilute phase and a phase separation interface which could affect momentum transfer, and (2) the viscous mean free path in the concentrated phase is an order of magnitude smaller than in the dilute phase which could explain a different sensitivity to, for instance, surface roughness.

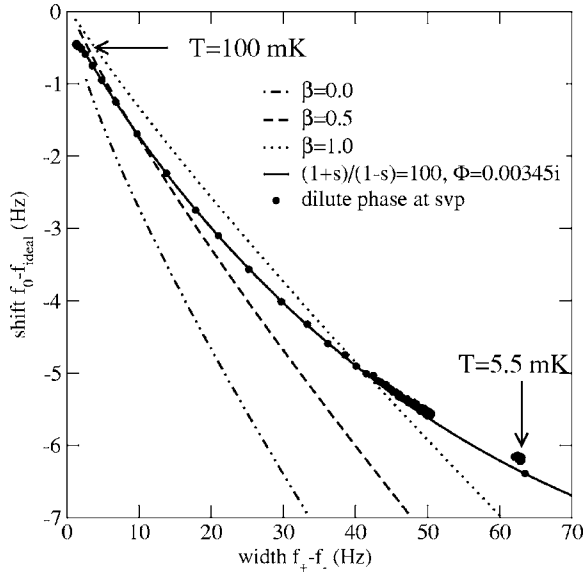


FIG. 3. The shift of the resonance frequency versus the resonance width of a PtRh viscometer with a vacuum resonance of $f_w = 944.351$ Hz in the dilute phase at svp. The dashed-dotted line is the solution of the Navier-Stokes equation and the dotted line is the theory of Høgaard Jensen *et al.* (Ref. 7) in the limit $\zeta \rightarrow \infty$. The dashed curve has been calculated on the basis of Eq. (8) with $\Phi = 0$ which corresponds to the hydrodynamic boundary condition $v_r(a) = 0$. The full curve has been calculated on basis of Eq. (8) with $(1+s)/(1-s) = 100$ and $\Phi = 0.00345i$ (calculated from the dilute phase properties and the frequency). Note, that $l_\eta/a \approx 0.8$ at the lowest temperatures.

V. VISCOUS MEAN FREE PATH RESULTS

The theory has been used to eliminate the slip effects in the analysis to measure the temperature dependence of the viscosity in the dilute and the concentrated phase at pressures of 0, 5, 7, 10, 12, 15, and 20 bars. The temperature has been measured by the melting curve thermometer and we have corrected the PLTS-2000 (Ref. 21) zero field melting curve for the changes due to the entropy reduction of the solid by the applied magnetic field assuming that the solid is a paramagnet. We found that a significant part of the pressure dependence of the viscosity is proportional to the density in the concentrated phase and to the normal density in the dilute phase. Therefore, we prefer to present the results as the viscous mean free path instead of the viscosity.

The low temperature dependence of the viscous mean free path in the dilute and concentrated phase including the leading order finite temperature correction is given by²²

$$\frac{1}{l_\eta T^2} = a - bT. \quad (12)$$

Figure 4 shows the results for the parameters a and b in the concentrated phase as a function of pressure. The closed and open circles are our results for a and b measured with a PtRh and a CuNi wire and the lines are linear fits to the results: $a(p) = a_1 p + a_0 \text{ m}^{-1} \text{ K}^{-2}$ and $b(p) = b_1 p + b_0 \text{ m}^{-1} \text{ K}^{-3}$ with p in bars. The constants are: $a_0 = (12.96 \pm 0.07) \times 10^9$, $a_1 = (0.979 \pm 0.006) \times 10^9$, $b_0 = (29.01 \pm 0.15) \times 10^9$, and b_1

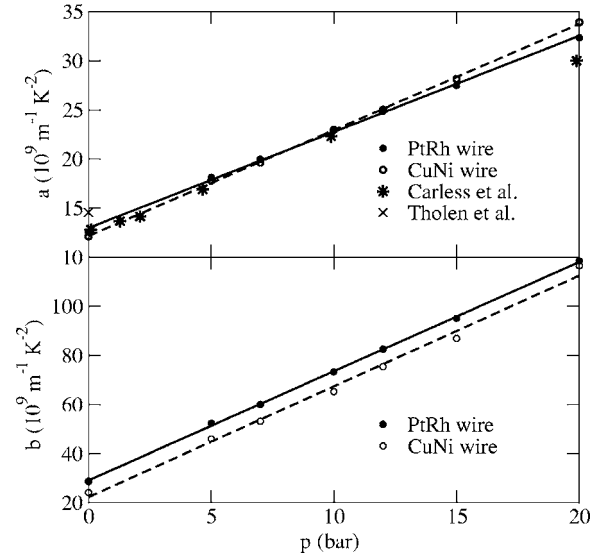


FIG. 4. The pressure dependence of the parameters a and b in Eq. (12) measured in the concentrated phase with a PtRh (full circles) and a CuNi wire (open circles). The lines are linear fit to the data. The stars represent the results for a given in Table I of Carless *et al.* (Ref. 12) converted to the viscous mean free path, including a correction of the temperature scale with a factor 0.89 (Ref. 17). The cross represents the summary of viscosity data at svp by Tholen *et al.* (Ref. 3).

$= (4.449 \pm 0.012) \times 10^9$ for the PtRh wire; and $a_0 = (12.14 \pm 0.04) \times 10^9$, $a_1 = (1.080 \pm 0.003) \times 10^9$, $b_0 = (22.20 \pm 0.62) \times 10^9$, and $b_1 = (4.513 \pm 0.053) \times 10^9$ for the CuNi wire. The error bars in the coefficients reflect the scatter of the data in Fig. 4.

The stars in Fig. 4 are the results for a given in Table I of Carless *et al.*¹² converted to the viscous mean free path, including the correction of the temperature scale of a factor 0.89 proposed by Greywall.¹⁷ The cross in Fig. 4 is the summary for viscosity data at SVP given by Tholen *et al.*³ converted to the viscous mean free path. We have also measured the viscosity at SVP in pure ^3He where the theory of Høgaard Jensen *et al.*⁷ is valid. The average over two CuNi viscometers and one PtRh viscometer (the resonance of the second PtRh viscometer was deformed) is $a = (12.28 \pm 0.10) \times 10^9 \text{ m}^{-1} \text{ K}^{-2}$ and $b = (23.9 \pm 1.0) \times 10^9 \text{ m}^{-1} \text{ K}^{-3}$. The agreement between our values of a obtained in the concentrated phase with a strong enhancement of the slip length and in pure liquid ^3He with a tiny enhancement of the slip length shows that the theory of Bowley and Owers-Bradley⁸ allows us to analyze viscometer data correctly when the scattering is almost entirely specular. The scatter in the values for a and b in the concentrated phase have a comparable contribution in the error bar on the viscosity at 50 mK. Furthermore, our values of a agree with the viscosity measurements by Carless *et al.*¹² but are significantly lower than the viscosity data summarized by Tholen *et al.*³

Figure 5 shows the results for the viscous mean free path in the dilute phase at SVP as a function of temperature, where the temperature has been measured by the melting curve thermometer. The scatter in the data at temperatures near 15 mK is due to the long thermal time constant of the

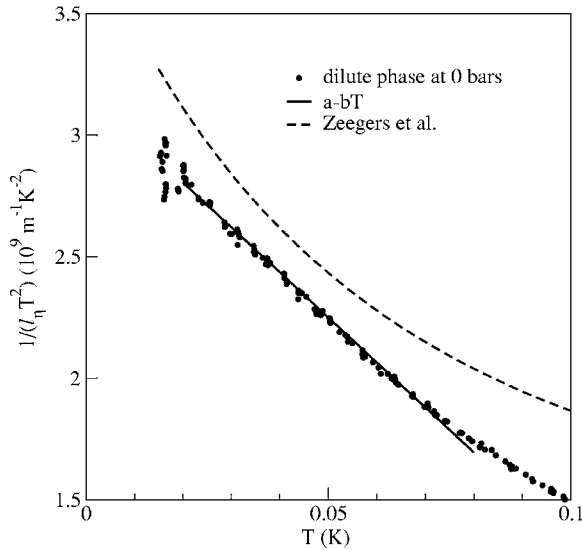


FIG. 5. The viscous mean free path in the dilute phase at 0 bars as a function of temperature. The full line is a fit of Eq. (12) to the data. The dashed line represents the fit by Zeegers *et al.* (Ref. 23) to their viscosity measurements to the viscous mean free path.

melting curve thermometer. Also shown are a fit of Eq. (12) to the data and the fit by Zeegers *et al.*²³ to their viscosity measurements converted to the viscous mean free path. Our result agrees better with Eq. (12) than the result published by Zeegers *et al.*²³

Figure 6 shows the pressure dependence of the parameters a and b measured with the PtRh wire in the dilute phase. The curves are polynomial fits to the results: $a(p) = a_2 p^2 + a_1 p + a_0 \text{ m}^{-1} \text{ K}^{-2}$ and $b(p) = b_2 p^2 + b_1 p + b_0 \text{ m}^{-1} \text{ K}^{-3}$ with p in bars and $a_0 = (3.239 \pm 0.009) \times 10^9$, $a_1 = (153.6 \pm 2.0) \times 10^6$,

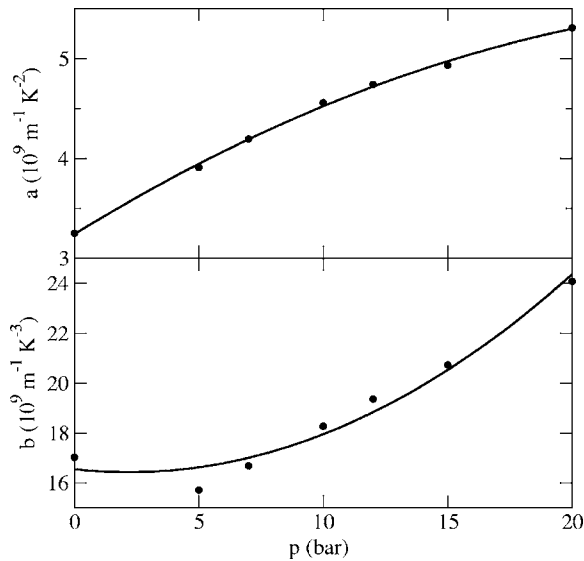


FIG. 6. The pressure dependence of the parameters a and b in Eq. (12) in the dilute phase. The curves are polynomial fits to the data: $a = ((-2.536 \pm 0.093) \times 10^6 p + (3.239 \pm 0.009) \times 10^9) p + (3.239 \pm 0.009) \times 10^9 \text{ m}^{-1} \text{ K}^{-2}$ and $b = ((25.0 \pm 1.7) \times 10^6 p + (-109.8 \pm 36.4) \times 10^6) p + (16.55 \pm 0.17) \times 10^9 \text{ m}^{-1} \text{ K}^{-3}$ with p in bars.

$$a_2 = (-2.536 \pm 0.093) \times 10^6, \quad b_0 = (16.55 \pm 0.17) \times 10^9, \quad b_1 = (-109.8 \pm 36.4) \times 10^6, \quad \text{and} \quad b_2 = (25.0 \pm 1.7) \times 10^6.$$

The analysis of the data in the dilute phase measured with the CuNi viscometer is difficult, because at low temperature β tends towards 0.2–0.3 which is outside the validity range of Eq. (8). We have inverted the experimental cell to compare the functionality of the CuNi viscometers in the dilute and concentrated phase. Both CuNi viscometers work well in the concentrated phase but show similar behavior for β in the dilute phase.

VI. SURFACE CONDITIONS

The agreement between theory and experiment depends on how careful a vibrating wire resonator has been mounted and is in general better for the PtRh wires than for the CuNi wires. The measurements of the resonance shift as a function of resonance width always show the tendency to curve as predicted by Eq. (8), but β tends to saturate at low temperatures to values in the range $0.4 < \beta < 0.5$ instead of 0.5. This effect is more pronounced for the CuNi wires in the dilute phase, where $0.2 < \beta < 0.3$.

There also remains the question why the enhancement of the slip length has not been observed in the viscometer experiments mentioned in the introduction. All three experiments use a ϕ 125 μm tantalum wire.^{4–6} Tentative application of Eq. (8) outside its validity range on one of those experiments²⁴ yields $(1+s)/(1-s) \approx 3$.

Einzel *et al.*¹³ have applied Eq. (5) on a mesoscopic scale to modelize the effect of surface roughness on slip enhanced by specular scattering. The roughness is modeled as a superposition of weak sinusoidal variations with wave number k and amplitude h . The theory is valid when $l_\eta \ll h, k^{-1} < \delta$, since the fluid flow near the surface is calculated hydrodynamically. The simplest approximation is to model the surface roughness by a single sinusoidal variation with amplitude h_S and wave number k_S . In the limit $k_S \zeta \gg 1$, the system behaves as if there is an effective slip length ζ_E given by

$$\frac{1}{\zeta_E} = \frac{1}{\zeta} + \frac{1}{\zeta_S}, \quad (13)$$

where $\zeta_S \approx 1/h_S^2 k_S^3$ is due to surface roughness. Applying this result to a wire, we would measure a roughness dependent β_S instead of the intrinsic β ,

$$\beta_S = \frac{\zeta_E}{2\zeta_E + a} = \frac{\zeta}{(2 + a/\zeta_S)\zeta + a}. \quad (14)$$

Figure 7 shows fits of Eq. (14) to data taken with a PtRh and a CuNi viscometer in the concentrated phase at $p=7$ bars. We find $\zeta_S = 32.9 \text{ m}$ for the PtRh wire and $\zeta_S = 107 \text{ m}$ for the CuNi wire.

Figures 8 and 9 show images made by a scanning electron beam microscope of the surface of our 25.7 μm PtRh wire and a 125 μm tantalum wire similar to the wire used in many other viscosity experiments in mixtures.^{4,23,25} The quality of the images of the CuNi wires suffer from charge effects because the wires are insulated, but they are clearly rougher than the PtRh wire and smoother than the tantalum wire. The

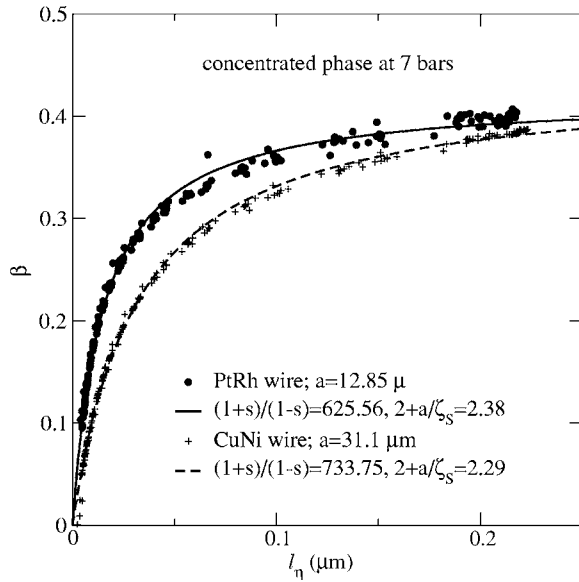


FIG. 7. The parameter β versus the mean free path for a PtRh and CuNi wire in the concentrated phase at $p=7$ bars. Fits of Eq. (14) to the data yield $\zeta_S=32.9$ m for the PtRh wire and 107 m for the CuNi wire.

characteristic length scale for the surface roughness is about 100 nm for the PtRh wire and $2 \mu\text{m}$ for the tantalum wire. Therefore, our experiment does not meet the condition $l_\eta \ll h, k^{-1}$ although not as badly in the concentrated phase as in the dilute phase. Indeed, the prediction $\zeta_S \approx 1/h_S^2 k_S^3$ and the observations $1/k_S=100/2\pi$ nm and $\zeta_S \approx 30$ m for the this PtRh wire would imply $h_S < 0.5$ nm. Figure 8 shows that h_S is 10–100 times as large. Nevertheless, it is possible that other surface mechanisms which reduce the slip length can lead to Eq. (13), but with a different physical interpretation

for ζ_S . For instance, Wang and Yu²⁶ have proposed that momentum transfer between the ^3He quasiparticles and a substrate covered with a ^4He rich boundary layer occurs via vortices threading the layer. Zwignagel and Toepffer²⁷ have calculated the slip in the flow of normal phase ^3He with a roughness smaller than the viscous mean free path and larger than the quasiparticle wavelength. In the case of pure specular scattering, they find a small enhancement of the slip length for a surfaces with a Gaussian distribution in height and slope which is several orders of magnitude smaller than the enhancement in our experiments.

Finally, the results for ζ_S in the concentrated phase are comparable for the CuNi and the PtRh viscometers. In the dilute phase, the values of ζ_S for the CuNi viscometers (about 25 m) are a factor 2–5 smaller than for the PtRh viscometers. A fundamental difference between the concentrated and dilute phase is that in the dilute phase the concentration changes from zero at the surface of the wire to its bulk value at a distance of several nanometers away¹ while in the concentrated phase the wire is surrounded by a thin layer of dilute phase and a phase separation interface. Surface tension may help to smooth out the surface roughness of the wire in the concentrated phase.

VII. CONCLUSION

The surface conditions for our vibrating wire viscometers have made it possible to observe two contributions to the slip in ^3He - ^4He mixtures. Specular scattering of the ^3He quasiparticles off the superfluid ^4He film adsorbed on the viscometers enhances the velocity slip in the tangential direction and renders the slip length in the hydrodynamic regime several orders of magnitude larger than the mean free path. The tangential slip is fully developed before the system reaches

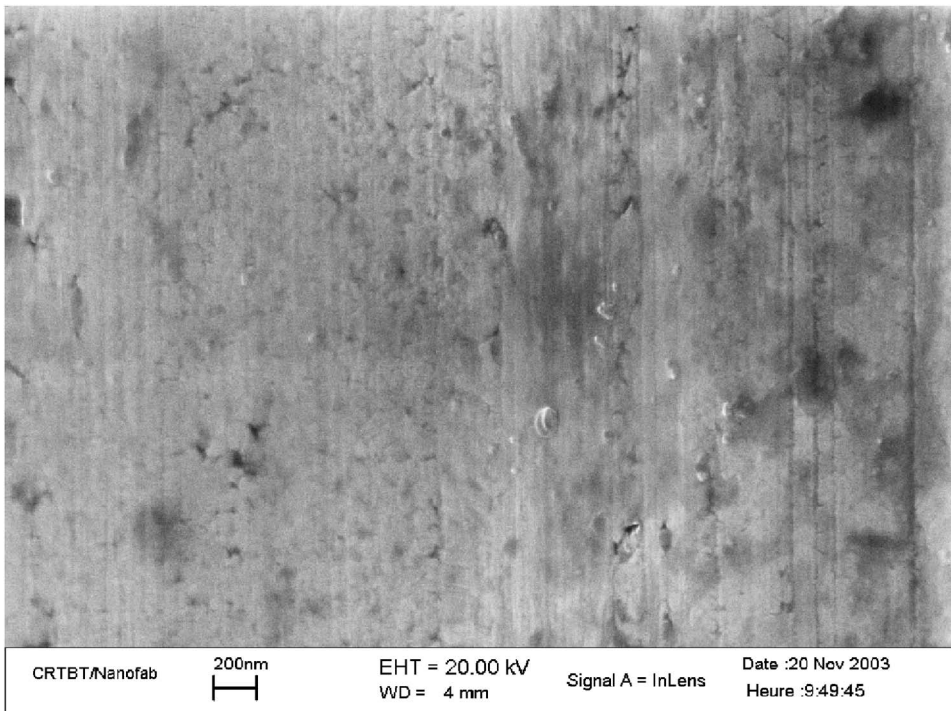


FIG. 8. Scanning electron beam microscope image of the $\phi 25.7 \mu\text{m}$ PtRh wire. The surface roughness has a characteristic wave vector length of about 100 nm and a characteristic amplitude of about 20 nm. The vertical scratches are probably due to the drawing of the wire.

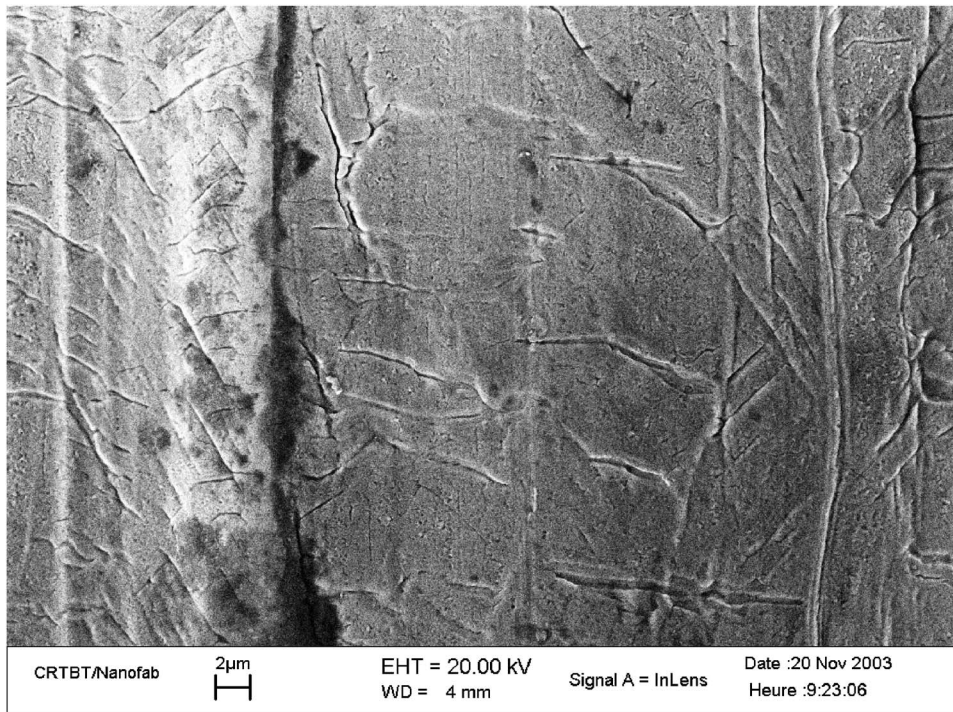


FIG. 9. Scanning electron beam microscope image of a ϕ 125 μm tantalum wire. The characteristic wavelength is estimated to be about 2 μm . The vertical scratches are probably due to the drawing of the wire.

the Knudsen regime. In this regime, we measure the effect of a velocity slip in the radial direction superimposed on the tangential velocity slip. Both contributions to the slip are in good agreement with the theory of Bowley and Owers-Bradley.⁸ We hope that the theory can be extended beyond its current validity limits, so that it can describe the behavior of a viscometer with a specular surface from the hydrodynamic regime to the ballistic limit.

ACKNOWLEDGMENTS

We are indebted to R. M. Bowley for sharing his ideas before publication and many fruitful exchanges. A. Sulpice has measured magnetization curves of the different wires at 1.7 K up to a field of 8 T and D. Bourgault has given us access to a superconducting magnet with a room temperature bore for quick characterization of the viscometers.

*Electronic address: gerard.vermeulen@grenoble.cnrs.fr

- ¹H. E. Hall, in *Liquid and Solid Helium*, edited by C. G. Kuper, S. G. Lipson, and M. Revzen (Wiley, New York, 1974), p. 375.
- ²D. A. Ritchie, J. Saunders, and D. F. Brewer, *Phys. Rev. Lett.* **59**, 465 (1987).
- ³S. M. Tholen and J. M. Parpia, *Phys. Rev. B* **47**, 319 (1993).
- ⁴A. M. Guénault, V. Keith, C. J. Kennedy, and G. R. Pickett, *Phys. Rev. Lett.* **50**, 522 (1983).
- ⁵J. Martikainen, J. Tuoriniemi, T. Knuuttila, and G. Pickett, *J. Low Temp. Phys.* **126**, 139 (2002).
- ⁶R. König and F. Pobell, *J. Low Temp. Phys.* **97**, 287 (1994).
- ⁷H. Højgaard Jensen, H. Smith, P. Wölfle, K. Nagai, and T. M. Bisgaard, *J. Low Temp. Phys.* **41**, 473 (1980).
- ⁸R. M. Bowley and J. R. Owers-Bradley, *J. Low Temp. Phys.* **136**, 15 (2004).
- ⁹S. Perisanu and G. Vermeulen, *J. Low Temp. Phys.* **134**, 701 (2004).
- ¹⁰S. Perisanu and G. Vermeulen, *J. Low Temp. Phys.* **138**, 19 (2005).
- ¹¹G. G. Stokes, *Mathematical and Physical Papers* (Cambridge University Press, London, 1901), Vol. III.
- ¹²D. C. Carless, H. E. Hall, and J. R. Hook, *J. Low Temp. Phys.* **50**, 583 (1983).
- ¹³D. Einzel, P. Panzer, and M. Liu, *Phys. Rev. Lett.* **64**, 2269 (1990).
- ¹⁴A. M. Guénault, V. Keith, C. J. Kennedy, S. G. Mussett, and G. R. Pickett, *J. Low Temp. Phys.* **56**, 511 (1986).
- ¹⁵D. S. Greywall and P. A. Bush, *J. Low Temp. Phys.* **46**, 451 (1982).
- ¹⁶J. P. Kauppinen, K. T. Loberg, A. J. Manninen, J. P. Pekola, and R. A. Voutilainen, *Rev. Sci. Instrum.* **69**, 4166 (1998).
- ¹⁷D. S. Greywall, *Phys. Rev. B* **33**, 7520 (1986).
- ¹⁸G. E. Watson, J. D. Reppy, and R. C. Richardson, *Phys. Rev.* **188**, 384 (1969).
- ¹⁹S. Yorozu, M. Hiroi, H. Fukuyama, H. Akimoto, H. Ishimoto, and S. Ogawa, *Phys. Rev. B* **45**, 12942 (1992).
- ²⁰A. Rodrigues and G. Vermeulen, *J. Low Temp. Phys.* **108**, 103 (1997).
- ²¹R. L. Rusby, M. Durieux, A. L. Reesink, R. P. Hudson, G. Schuster, M. Kühne, W. E. Fogle, R. J. Soulen, and E. D. Adams, *J. Low Temp. Phys.* **126**, 633 (2002).
- ²²K. S. Dy and C. J. Pethick, *Phys. Rev.* **185**, 373 (1969).
- ²³J. C. H. Zeegers, A. T. A. M. de Waele, and H. M. Gijssman, *J. Low Temp. Phys.* **84**, 37 (1991).
- ²⁴R. König, Ph.D. thesis, Universität Bayreuth (1993).
- ²⁵R. König and F. Pobell, *Phys. Rev. Lett.* **71**, 2761 (1993).
- ²⁶C. Wang and L. Yu, *Physica B* **169**, 529 (1991).
- ²⁷G. Zwignagel and C. Toepffer, *Phys. Rev. B* **45**, 8138 (1992).